Stress analysis around a through crack in a thin copper film using molecular dynamics

D. Johansson[1], P. Hansson[2] and S. Melin[3]

[1] Division of Mechanics, Department of Mechanical Engineering, Lund University, P.O. Box 118, 22100 Lund, Sweden, dan.johansson@mek.lth.se
[2] per.hansson@mek.lth.se
[3] solveig.melin@mek.lth.se

ABSTRACT. *A small rectangular strip of FCC Cu, containing a through crack on the nano-scale and subjected to loading under displacement control, is simulated using molecular dynamics. The geometry is used to mimic that of a thin film between two stiff layers and therefore the height of the rectangle is much smaller than the width. A plain strain situation is modeled by applying periodic boundary conditions in the direction of the crack front. The Lennard-Jones pair potential is used for the inter-atomic forces. The centrally placed crack is created by removing a few atoms inside the specimen. The crack will be loaded perpendicular to the crack plane and comparisons with traditional linear elastic fracture mechanics concepts will be made. The ultimate goal is to find a limit in model size beneath which linear elastic fracture mechanics measures looses their meaning.*

INTRODUCTION

Components with one or more linear measures on the nanometer scale are nowadays part of everyday life, Devices on this scale can, with technology of today, be produced with very high accuracy. Thus, the applications within a variety of technological fields are a fact. Examples can be found in medical devices as well as in electromechanical circuits. One example within medicine is the use of small, resonant beams, of length perhaps one hundred micrometers but with cross section measures about one micrometer, only. By covering of such a beam by a thin layer, of a few nanometers in thickness only, of a material that reacts to specific biomarkers in the surrounding, the concentration of such markers can be detected through a shift in eigenfrequencies of the beam. Another common application is within nano-electro-mechanical systems, NEMS, where layers of thicknesses down to a few nanometers are utilized for insulting/conductive purposes, or simply as a protective coating layer. We are in everyday life surrounded by structures where behaviour and functions are determined at the atomistic level [1,2].

It is well established that structures on the nanometer scale show material properties and behavior that differ from components at the macroscopic scale. This is due to factors as the increasing number of surface atoms in relation to number of bulk atoms

with decreasing size, the fewer number of grains, and due to this the relatively lower dislocation density as compared to macroscopic structures. Also crystallographic factors, such as crystal orientation, strongly influence the material properties; cf. e.g. [3,4].

As regards thin metallic layers, one difficulty lies in finding proper dimensioning rules that are scientifically based and commonly accepted among designers. One such challenge is the prediction of sudden failure of the layer due to crack propagation induced by mechanical loading. Even if the crack is only a few nanometers, it might jeopardize the functionality of the coating and, eventually, extend to cause structure breakdown. Such events are, of course, necessary to understand and be able to predict. In this paper, a thin strip of Cu, with height of only a few nanometers and holding a centrally placed crack loaded perpendicular to the crack plane by displacement control will be investigated by molecular dynamics (MD) simulations using an in-house code. The results will be compared to traditional linear elastic fracture mechanics (LEFM) solutions to judge the impact of size.

PROBLEM SPECIKICATION

The objective of this investigation is a thin strip of Cu, holding a centrally placed crack along the x-direction according to Figure 1. The crack is loaded perpendicular to the crack plane under displacement control. Coordinate directions (x, y, z) are shown in Figure 1 together with local coordinates (r, θ) at the crack tip.

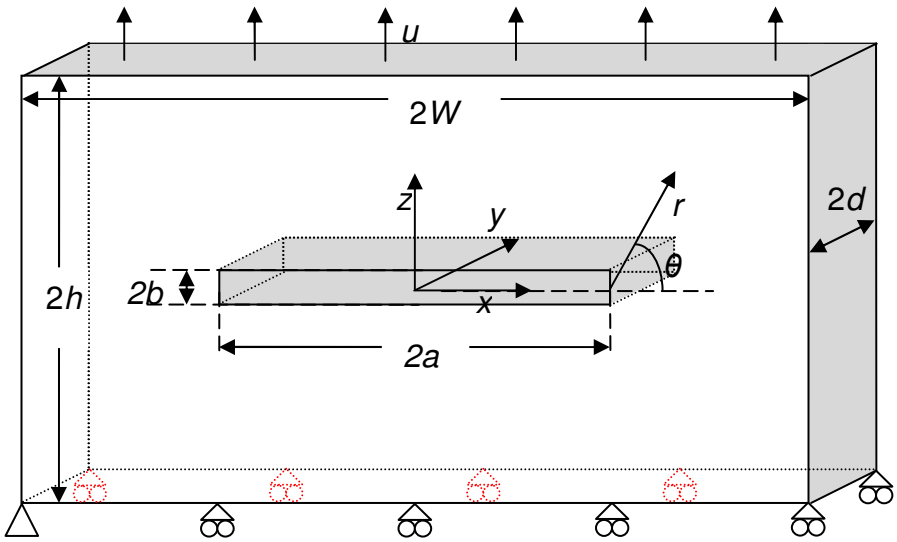

Figure1. Model configuration. The crack is modelled rectangular of size 2*a*x2*b*.

The atomic arrangement is FCC Cu unit cells with lattice constant a_0. The height of the strip in the z-direction is 2*h*, the width in the x-direction 2*W* and the thickness in the y-direction is 2*d*. The basic model comprises six unit cells in the y-direction so that 2*d* =

$6a_0$. By imposing periodic boundary conditions in the y-direction, a state of plane strain is reached.

The crack is introduced by removing a strip of height two unit cells along the crack line, giving a rectangular crack shape with length $2a$ and height $2b = 2a_0$. The boundary conditions at the bottom of the strip are realized by preventing movement of all atoms in the bottom atom layer in the z-direction together with locking the leftmost corner atom at the bottom atom layer in all directions. Displacement control is imposed by moving all atoms in the two top atom layers at the top of the strip simultaneously at equal velocity in the [0 0 1] direction. No boundary conditions are imposed at the sides of the strip so that contraction in the x-direction can take place.

THEORY

Here the Lennard-Jones 12-6 pair potential is employed, cf. [5]. The expression reads

$$\phi = 4\alpha\left[\left(\frac{\beta}{r}\right)^{12} - \left(\frac{\beta}{r}\right)^{6}\right] \tag{1}$$

In the Lennard-Jones potential the r-12-term describes the electron orbital overlapping causing a short ranged repulsive force, i.e. the Pauli repulsion, while r-6-term describes the dispersion force which is a long ranged attracting force. The constants α and β in Eq. (1) are the depth of the potential well and the distance at which the inter-particle potential equals zero, respectively. The distance defined by β also marks the length scale [5,6].

The Cauchy stress tensor σ for an atomistic ensemble region with volume V can be described as:

$$\boldsymbol{\sigma} = \begin{pmatrix} \sigma_{xx} & \sigma_{xy} & \sigma_{xz} \\ \sigma_{yx} & \sigma_{yy} & \sigma_{yz} \\ \sigma_{zx} & \sigma_{zy} & \sigma_{zz} \end{pmatrix} = -\frac{1}{2V}\sum_i \sum_{j\neq i} \boldsymbol{r}_{ij} \otimes \boldsymbol{f}_{ij} \tag{2}$$

Here $\boldsymbol{r}_{ij} = \boldsymbol{r}_j - \boldsymbol{r}_i$, where $\boldsymbol{r}_i$ and $\boldsymbol{r}_j$ denotes the positions for atom i and j, respectively, and

$$\boldsymbol{f}_{ij} = -\frac{\partial\phi(r_{ij})}{\partial r_{ij}}\frac{\boldsymbol{r}_{ij}}{r_{ij}} \tag{3}$$

with $r_{ij} = |\boldsymbol{r}_{ij}|$ [7]. The stresses calculated from Eq. (2) will be compared to linear elastic fracture mechanics solutions.

SIMULATION PROCEEDURE

In this paper the stress distributions for two different geometries, G1 and G2, are presented, cf. Table 1 for simulation data. Each MD simulation comprises three phases; problem setup, relaxation and loading.

During the problem setup phase all specific simulation parameters according to Table 1 are imposed. The atomic arrangement is generated, atoms are removed to form the crack, and the boundary conditions are imposed.

Table 1. Simulation parameters for geometries G1 and G2.

	G1	G2
Strip size 2*W*x2*h* [unit cells]	80x20	20x10
Crack size 2*a*x2*b* [unit cells]	24x2	6x2
Number of atoms [-]	37248	4512
Total number of time steps [-]	48000	40000
Number of relaxation steps [-]	12000	8000
Strain rate [s^{-1}]	$1.14 \cdot 10^8$	$1.17 \cdot 10^8$
Final strain ε_{max} [%]	7.0	6.4
Time step [fs]	17	17
Time step [fs]	17	17
Temperature *T* [K]	0.001	0.001

In the second phase, the relaxation phase, a chosen temperature is assigned. This is done by energy dissipation by multiplying the velocity of each atom with a scaling factor every two-hundred time step. Before the multiplication, the velocities of the atoms are updated. The magnitude of the scaling factor is determined by a Riemann sum of the mean value of the squared velocity. During the relaxation phase the strip in terms of size and volume moves towards a steady state, where the internal stress components only oscillates slightly around zero so that the relation between potential and kinetic energies keeps constant to a chosen magnitude of accuracy. Further, during relaxation, the two top atomic layers movements are restricted so that the top surface atom layer remains plane, in parallel with the *xy*-plane. This is imposed by initially putting all velocities equal to zero and then give the same acceleration all atoms in two top layers in the z-direction. The assigned acceleration equals the mean of all the two top layer atom accelerations in the z-direction.

After that the strip has remained in steady state for a few thousand time steps, the loading phase is entered and the two top atom layers are given a constant velocity in positive z direction causing a controlled displacement , i.e. displacement control is imposed.

Material related parameters are given in Table 2. It should be noted that the chose values of α, β, and r_c are not always preferred. The present choice stems from [8] and provides a better agreement with the Young's modulus *E*.

Table 2. Material related parameters [8,9].

Lattice constant a_0 [nm]	0.36	Potential well depth α [eV]	0.1515
Young's modulus *E* [GPa]	110	Distance for zero potential β [nm]	0.2338
Poisson's ratio ν [-]	0.34	Cut-off radius r_C (2.74 β) [nm]	0.6406

RESULTS AND DISCUSSION

During the initial relaxation, both geometries were reduced in volume; G1 by 6.4% and G2 by 6.8%. In the z-direction the height was reduced by approximately 3.2% for both geometries. From this relaxed stage, loading was pursued until a maximum strain, ε_{max}, was reached. At this strain the atomic arrangements still behaved elastic, with no signs of plasticity in terms of dislocation formation.

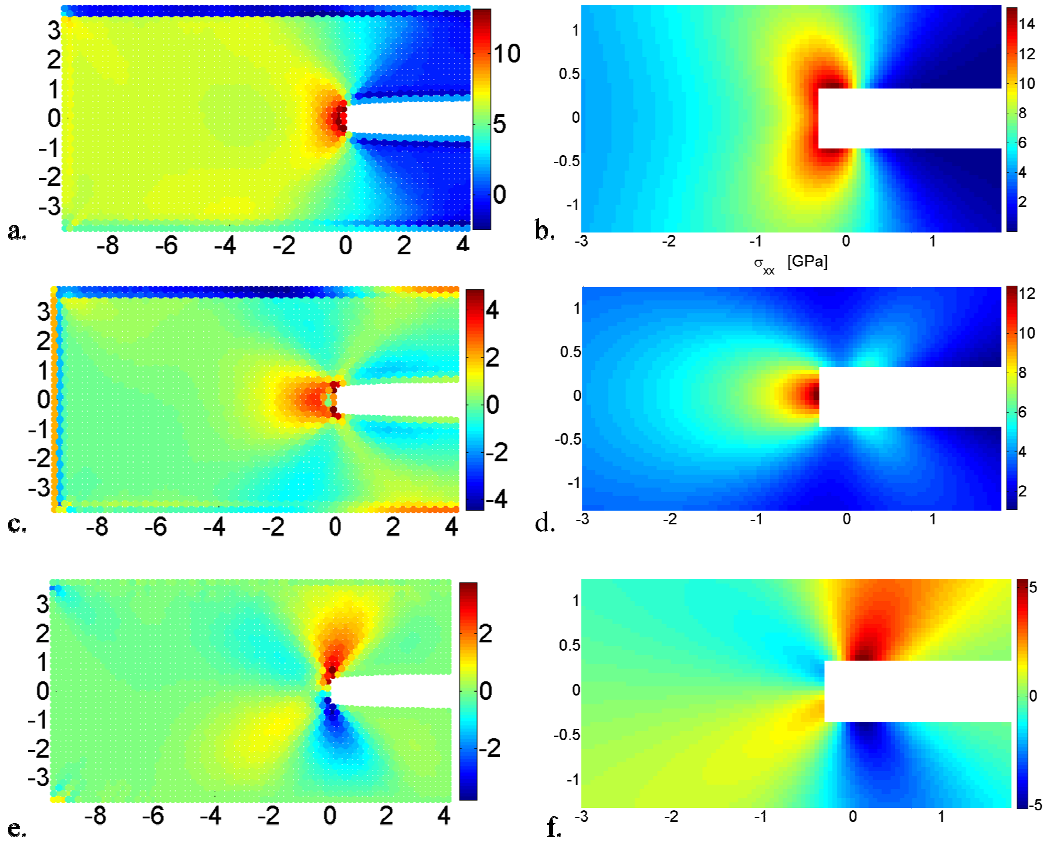

Figure 2. σ_{zz},, σ_{xx} and σ_{zx} in the crack tip vicinity for G1. Abscissa and ordinate are given in [nm]. The bars are in [GPa]. a,c,e: MD simulations. b,d,f: LEFM solutions.

In Figure 2 stresses for the larger geometry G1 are shown at maximum strain. Figure 2a,c,e show the outcome from the MD simulation, and Figure 2b,d,f the LEFM solutions for an infinitely sharp crack in a displacement loaded finite strip as taken from [10]. The stresses in Figure 2b,d,f are displayed, with the exclusion of an area of height $2a_0$ around the crack and with the infinitely sharp crack marked by a sold line, in similarity to Figure 2a,c,e from the MD simulation. Note that the length scales differ between the presentation of the MD and LEFM results, and in Figure 2a,c,e the areas for which the linear elastic solutions in Figure 2b,d,f are shown, are framed. Also note that for the MD simulation, the entire height of the strip, 2h, is displayed. Further, in Figure

3a, ahead of the crack tip at θ = 0, cf. Figure 1, taken from Figure 2a and Figure 2c, are drawn. Figure 3b is a magnification of the MD values in Figure 3a. Corresponding results for geometry G2 are found in Figure 4 and Figure 5.

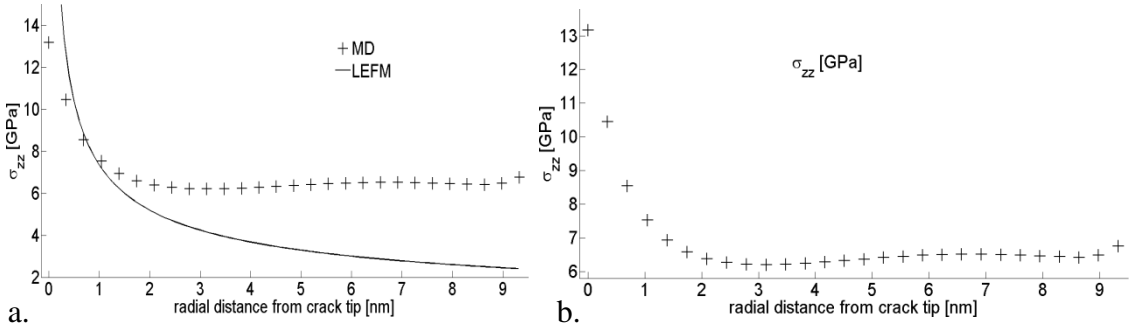

Figure 3. σ_{zz} ahead of the crack tip for G1. The abscissa is in [nm] and the ordinate in [GPa]. + show MD results and the solid line the LEFM solution. b) is a magnification of the MD values in a).

First consider the results concerning the largest geometry, G1, in Figure 2 and Figure 3. In general terms the stress fields agree in shapes and trends between the MD simulation and the LEFM solution. As expected, the sharp crack gives higher stress levels than the square shaped crack in the MD simulation. The stress levels of σ_{zz} as obtained from the MD (+) and LEFM (__) calculations are seen in Figure 3a, and Figure 3b is a close-up of the MD simulation values. Aside from the higher stress magnitude for the LEFM simulation, σ_{zz} from the MD simulation shows a singular behavior as the crack front is approached as seen from Figure 3b. This is expected due to the sharp corners forming the molecular crack front.

Further it is seen from Figure 2 that the boundary is affecting the stress distributions ahead of the crack front as compared to the LEFM solutions. As regards the MD shear stress distribution, each of the two corners of the crack front induces areas of enhanced magnitudes of σ_{zx}, both above and below the crack. The stress field seems to be composed by a superposition of two stress fields, emanating from the two stress concentrations at the corner points, each acting as a crack tip, but of lower singularity. These bands of enhanced shear stress might act as sites of dislocation nucleation.

Turning to the smaller geometry G2 in Figure 4 and Figure 5, it is noticed that all effects found for G1 are enhanced for G2. Still there is a resemblance between the MD and LEFM stress fields, but the inference from the boundaries have increased dramatically. This is also obvious from Figure 5b, where σ_{zz}, after having shown a singular behavior close to the crack front for $\theta = 0$, eventually increases as the distance to the boundary decreases.

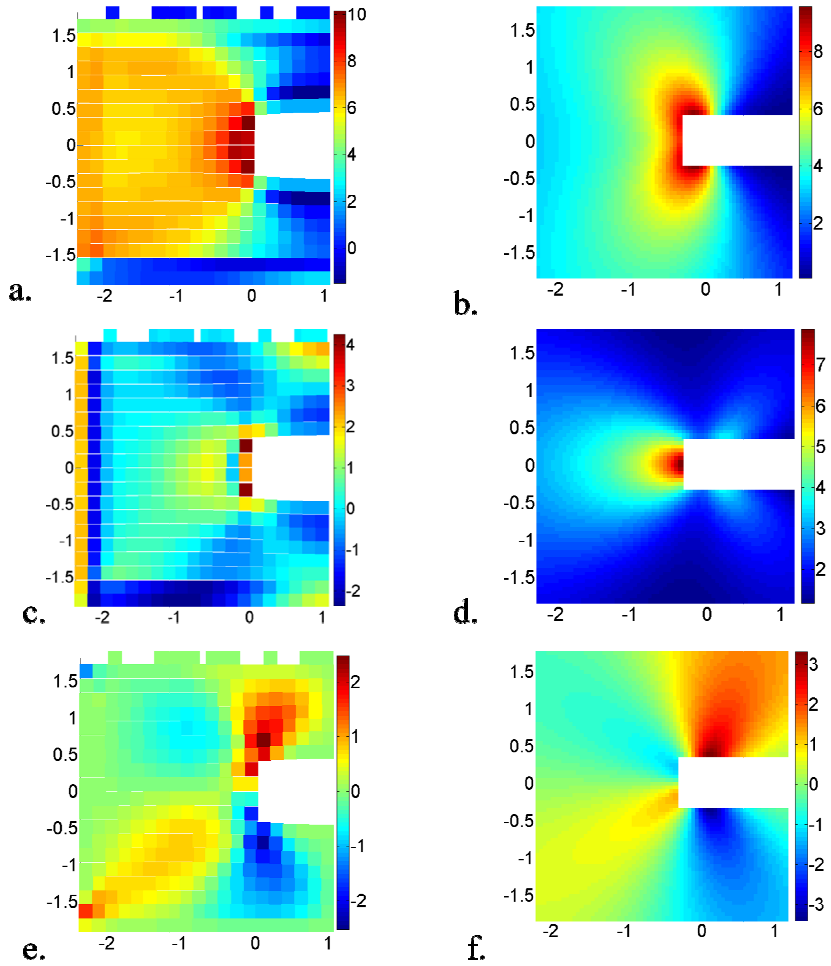

Figure 4. σ_{zz},, σ_{xx} and σ_{zx} in the crack tip vicinity for G2. Abscissa and ordinate are given in [nm]. The bars are in [GPa]. a,c,e: MD simulations. b,d,f: LEFM solutions.

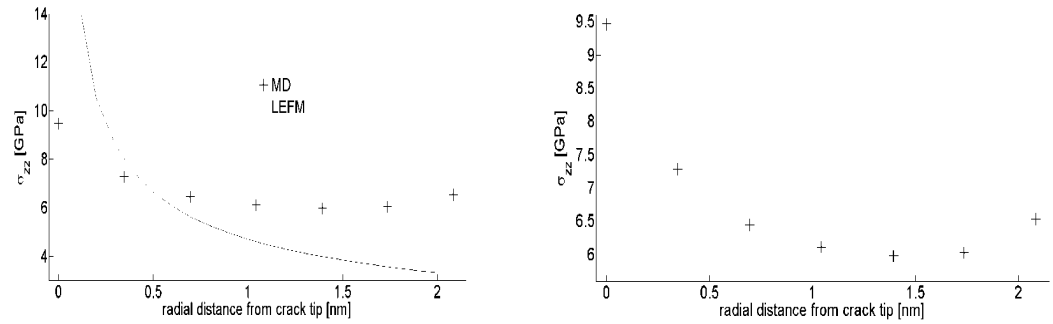

a. b.

Figure 5. σ_{zz} ahead of the crack tip for G2. The abscissa is in [nm] and the ordinate in [GPa]. + show MD results and solid line the LEFM solution. b) is a magnification of the MD values in a).

CONCLUSIONS

Molecular dynamics simulations have shown that cracked layers of small enough size react differently than macroscopic components upon loading. In this investigation, displacement controled loading of cracked layers of Cu, with layer thicknesses of a few nanometers, were considered. The stress field obtained from the MD simulations were compared to LEFM continuum solutions.close to the crack front.

The stress fields as determined from MD and LEFM continuum solutions were, in this study, shown to increasingly deviate as the layer thickness decreased. Evenso, the general appearence of the stress dstributions was kept. The influence from boundaries increased markedly as the layer thickness decreased.

REFERENCES

1. B. Ilic, Y. Yang and H.G. Craighead: Virus detection using nanoelectromechanical devices, J. Appl. Phys. Vol 85-2604 (2004)
2. D.H. Reich, M. Tanase, A. Hultgern, L.A. Bauer, C.S. Chen et al.: Biological applications of multifunctional magnetic nanowires, J. Appl. Phys. Vol. 93-7275 (2003)
3. P. Olsson, S. Melin and C. Persson: Atomistic simulations of tensile and bending properties of single-crystal bcc iron nanobeams, Phys. Rev. B 76, 224112 (2007)
4. P. Olsson and S. Melin, in Atomistic studies of the elastic properties of metallic BCC nanowires and films, edited by R Pyrz and J C Rauhe IUTAM Symposium on Modelling Nanomaterials and Nanosystems (2008), p.221-230
5. J.E. Jones: On the Determination of Molecular Fields, Proc. R. Soc. Lond. A Vol. 106 (1924), p. 463-477
6. D.C. Rapaport: The Art of Molecular Dynamics (Cambridge University Press, UK 2004).
7. M. Zhou: A new look at the atomic level virial stress: on continuum-molecular system equivalence, Proc. R. Soc. Lond. A Vol 459 (2003), p. 2347-2392
8. G. Ziegenhain, A. Hartmaier and H.M. Urbassek: Pair vs many-body potentials: Influence on elastic and plastic behavior in nanoindentation of fcc metals, J. Mech Phys. Solids Vol. 57, 1514-1526, (2009)
9. D.R. Askeland: The Science and Engineering of Materials (Chapman & Hal,l UK/China 1996).
10. M. Isida: Effect of width and length on stress intensity factors of internally cracked plates under various boundary conditions, Int. J. Fract. Mech. 7 (1971) p 301.